www.czasopisma.pan.pl PAN www.journals.pan.pl

jet INTL JOURNAL OF ELECTRONICS AND TELECOMMUNICATIONS, 2022, VOL. 68, NO. 4, PP. 831–840
Manuscript received July 15, 2022; revised November, 2022. DOI: 10.24425/ijet.2022.143892

Low Complexity Multiplier-less Modified FRM Filter Bank using MPGBP Algorithm

A. K. Parvathi, and V. Sakthivel

***Abstract*—The design of a low complexity multiplier-less narrow transition band filter bank for the channelizer of multi-standard software-defined radio (SDR) is investigated in this paper. To accomplish this, the modal filter and complementary filter in the upper and lower branches of the conventional Frequency Response Masking (FRM) architecture are replaced with two power-complementary and linear phase filter banks. Secondly, a new masking strategy is proposed to fully exploit the potential of the numerous spectra replicas produced by the interpolation of the modal filter, which was previously ignored in the existing FRM design. In this scheme, the two masking filters are appropriately modulated and alternately masked over the spectra replicas from 0 to 2π, to generate even and odd channels. This Alternate Masking Scheme (AMS) increases the potency of the Modified FRM (ModFRM) architecture for the design of computationally efficient narrow transition band uniform filter bank (termed as ModFRM-FB). Finally, by combining the adjoining ModFRM-FB channels, Non-Uniform ModFRM-FB (NUModFRM-FB) for extracting different communication standards in the SDR channelizer is created. To reduce the total power consumption of the architecture, the coefficients of the proposed system are made multiplier-less using Matching Pursuits Generalized Bit-Planes (MPGBP) algorithm. In this method, filter coefficients are successively approximated using a dictionary of vectors to give a sum-of-power-of-two (SOPOT) representation. In comparison to all other general optimization techniques, such as genetic algorithms, the suggested design method stands out for its ease of implementation, requiring no sophisticated optimization or exhaustive search schemes. Another notable feature of the suggested approach is that, in comparison to existing methods, the design time for approximation has been greatly reduced. To further bring down the complexity, adders are reused in recurrent SOPOT terms using the Common Sub-expression Elimination (CSE) technique without compromising the filter performance.**

***Keywords*—Frequency response masking (FRM), Modified FRM filter bank (ModFRM-FB), Multiplier-less filter, Matching pursuits with generalized bit planes (MPGBP), Sum-of-power-of-two (SOPOT), Common sub-expression elimination (CSE)**

I. Introduction

THE The Frequency Response Masking (FRM) method (1) has proven to be an effective method for realizing arbitrary bandwidth narrow transition width digital filters with less number of multipliers. Following Y.C. Lim's pioneer work on FRM, a great deal of research has been done in this area. Although these updated FRM techniques introduced a sharp finite impulse response (FIR) filter design with lesser multiplier complexity, the filter bank (FB) design from FRM architecture will need a set of complex band-pass masking filters. To take advantage of FRM architecture in the design of FBs, several works have come up in which the prototype filter is designed using FRM technique (2; 3; 4; 5; 6). The hardware complexity of these systems was further reduced by replacing the multipliers with basic shifters and adders/subtractors (7; 8; 9; 10) or using intelligent optimization methods (11; 12) at the cost of a slight frequency response degradation within a certain ripple margin (13). However, these algorithms suffer from large design time due to huge search space or slow convergence due to the time it takes to find local minima. Therefore, it is more viable to establish a trade-off between the approximation accuracy and the design time.

A low complexity reconfigurable FB for software-defined radio (SDR) channelizer was recently suggested by us in (14). In this work, the classical FRM structure was remodeled by replacing the modal filter and complementary filter with two power-complementary and linear phase filter banks. This advanced architecture (termed as Modified FRM (ModFRM)) permits the computationally efficient generation of narrow transition band uniform filter bank (termed as UModFRM-FB). In this method, the spectral replicas of the interpolated modal filter that was masked out in the conventional FRM approach are most effectively used by the newly proposed masking scheme without increasing the computational complexity. The proposed ModFRM design is made multiplier-less based on Matching Pursuits Generalized Bit-Plane (MPGBP) algorithm (15). This algorithm helps us to build the representation dictionary while keeping the design complexity minimal. The proposed design is notable for its ease of implementation, which eliminates the need for sophisticated optimization or exhaustive search methods. It enables the realization of impulse response coefficients that meets the prescribed specifications in the smallest number of signed sums of powers of two (SOPOT) terms, reducing the number of adders. The adder cost is further reduced using the Common Sub-expression Elimination (CSE) algorithm (16; 17). The major research contributions of this work are summarized as follows:-

- A very low complexity multiplier-less narrow transition band Modified FRM filter bank for use in the channelizer of multi-standard SDR is investigated.
- The suggested multiplier-less design has reduced complexity than previous approaches, making it a superior alternative for channel filters in SDR receivers.

Authors are with National Institute of Technology, Calicut, India (e-mail: parvathiak92@gmail.com, sakthi517@nitc.ac.in).

- The proposed multiplier-less ModFRM design using the MPGBP algorithm has the advantage of not imposing a fixed number of adders for each coefficient. This eliminates the flaw in traditional search algorithms, which usually assign too many or too few signed power-of-two (SPT) terms to a coefficient.
- The recommended design method stands out from all other generic optimization strategies, such as genetic algorithms, for its ease of implementation as it needs no specialized optimization or exhaustive search procedures.
- The design time for the approximation is considerably reduced as a result of this.

The rest of the paper is structured as: Section II begins with an outline of the conventional FRM architecture and goes in-depth into the design of ModFRM-FB using the Alternate Masking Scheme (AMS). The proposed design of multiplier-less ModFRM-FB using MPGBP and the optimization of the adder cost by CSE algorithm is given in Section III. The result analysis is presented in Section IV. The paper comes to a close with Section V.

II. Modified FRM Filter Bank based on Alternate Masking Scheme

The elegance of the conventional FRM architecture is that it divides the design of a higher-order filter into four sub-filters: the modal filter $H_a(z)$, complementary filter $H_c(z)$, masking filter $H_{Ma}(z)$, and complementary masking filter $H_{Mc}(z)$, all of which have lower design criteria.

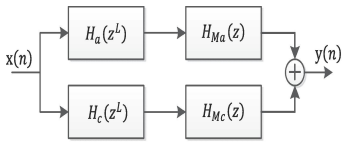

Fig. 1. Conventional FRM structure

The sharp filter is constructed by cascading the interpolated modal filter, also referred as band-edge shaping (BES) filter, and its complementary filter with the two masking filters, as shown in Figure 1. Here L denotes the factor of interpolation. Figure 2 shows a frequency response depiction of the FRM technique. The difference between Case I and Case II is that in the former, $H_a(z^L)$ determines the frequency response of the overall filter near the transition band, while in the latter, $H_c(z^L)$ does. Mathematically, FRM filter is represented as,

$$H(z) = H_a(z^L)H_{Ma}(z) + H_c(z^L)H_{Mc}(z) \tag{1}$$

where $H_c(z)$ is attained as:

$$H_c(z) = z^{-(N-1)/2} - H_a(z) \tag{2}$$

Here N is the length of the modal filter.

Figure 3 illustrates the ModFRM architecture. A power-complementary and linear phase FB replaces the modal and complementary filters in the conventional FRM structure. Initially, a lower-order modal filter, $H_a(z)$ of appropriate passband and transition width is modulated over the entire spectrum to get a set of band-pass filters. Each modulated

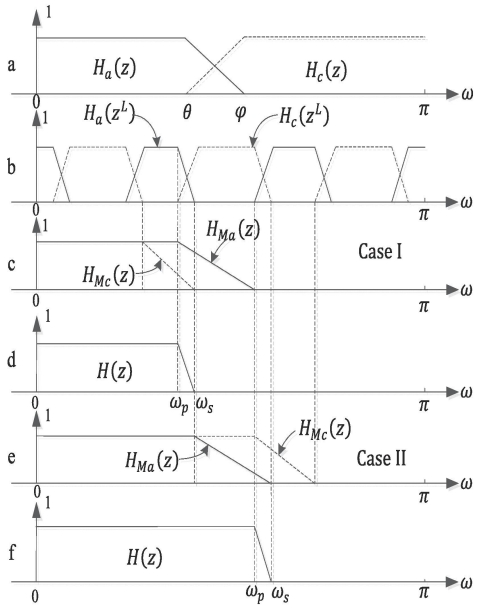

Fig. 2. Frequency response depiction of the conventional FRM structure

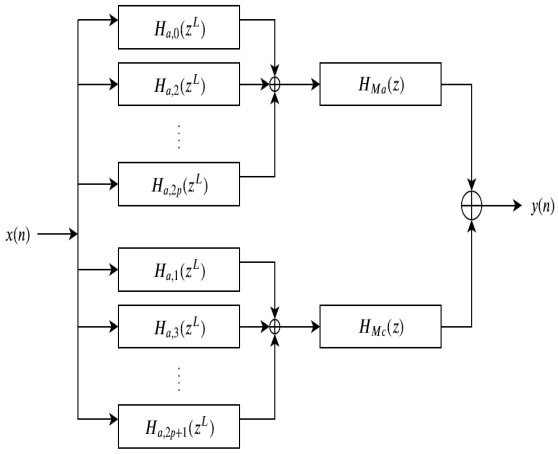

Fig. 3. Proposed ModFRM prototype filter

version is then interpolated by an interpolation factor of L. The role of the $H_a(z^L)$ and $H_c(z^L)$ in classical FRM is taken by the sum of interpolated even modulated channels named as even band-edge shaping filter bank (even BES-FB) and the sum of interpolated odd modulated channels named as odd band-edge shaping filter bank (odd BES-FB), respectively. It is then cascaded with the masking filters as shown in Figure 3 to generate the ModFRM prototype filter. The number of modulated filters, m must be odd such that the frequency response occurs alternately when the modulated filters are recombined. Therefore,

$$m = 2p + 1; p = 0, 1, 2.. \tag{3}$$

To ensure complete spectral coverage by the modal filter and its m modulated filters, passband, and stopband edge frequencies of the modal filter, ρ and ς should satisfy the condition:

$$(m + 1)(\rho + \varsigma) = 2\pi \tag{4}$$

In addition, the transition band of $H_a(z)$ must fulfill the power-complementary condition so that the even BES-FB and odd BES-FB will form linear phase FB with power-complementary property.

The transfer function of the ModFRM prototype filter can be written as:

$$H(z) = [H_{a,0}(z^L) + H_{a,2}(z^L) + ... + H_{a,2p}(z^L)]H_{Ma}(z) + [H_{a,1}(z^L) + H_{a,3}(z^L) + ... + H_{a,2p+1}(z^L)]H_{Mc}(z) \quad (5)$$

where $H_{a,q}(z^L)$ represents the q^{th} DFT modulated modal filter interpolated by a factor L.

The frequency response of the overall filter near the transition band can be determined either by even BES-FB or odd BES-FB. Accordingly, the design specifications of the masking filters can be computed as:

Case I

$$\omega_{p,Ma1} = \frac{3\rho + 2\varsigma}{L}; \omega_{s,Ma1} = \frac{4\rho + 3\varsigma}{L};$$
$$\omega_{p,Mc1} = \frac{\rho + 2\varsigma}{L}; \omega_{s,Mc1} = \frac{2\rho + 3\varsigma}{L};$$

Case II:

$$\omega_{p,Ma2} = \frac{\varsigma}{L}; \omega_{s,Ma2} = \frac{\rho + 2\varsigma}{L};$$
$$\omega_{p,Mc2} = \frac{2\rho + \varsigma}{L}; \omega_{s,Mc2} = \frac{3\rho + 2\varsigma}{L}; \quad (6)$$

From (6), it can be deduced that for large values of L, higher-order sharp masking filters will be required due to the denser replicas in the even and odd BES-FB. To overcome this difficulty, the masking filters are implemented using a simpler variant of FRM, called interpolated FIR (IFIR) technique (18). The IFIR structure is the cascade of two filters: IFIR modal filter and the image-suppressor filter. The optimal interpolation factor, L_{IFIR}, for minimum multipliers is chosen as:

$$L_{IFIR} = \frac{2\pi}{\omega_{p,Ma} + \omega_{s,Ma} + \sqrt{2\pi(\omega_{s,Ma} - \omega_{p,Ma})}} \quad (7)$$

The passband and stopband edge frequencies of IFIR modal filter and image-suppressor filter for $H_{Ma}(z)$ is calculated as follows:

$$\omega_{p,modal} = L_{IFIR} \times \omega_{p,Ma} \quad (8)$$

$$\omega_{s,modal} = L_{IFIR} \times \omega_{s,Ma} \quad (9)$$

$$\omega_{p,suppressor} = \omega_{p,Ma} \quad (10)$$

$$\omega_{s,suppressor} = \frac{2}{L_{IFIR}} - \omega_{s,Ma} \quad (11)$$

The edge frequencies of the subfilters for $H_{Mc}(z)$ can also be calculated similarly.

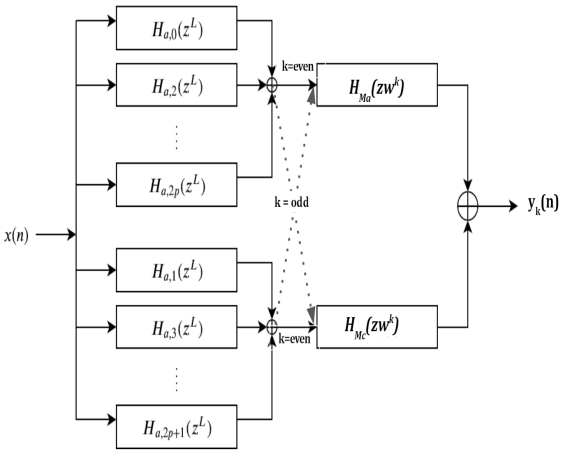

Fig. 4. Proposed ModFRM-FB using AMS

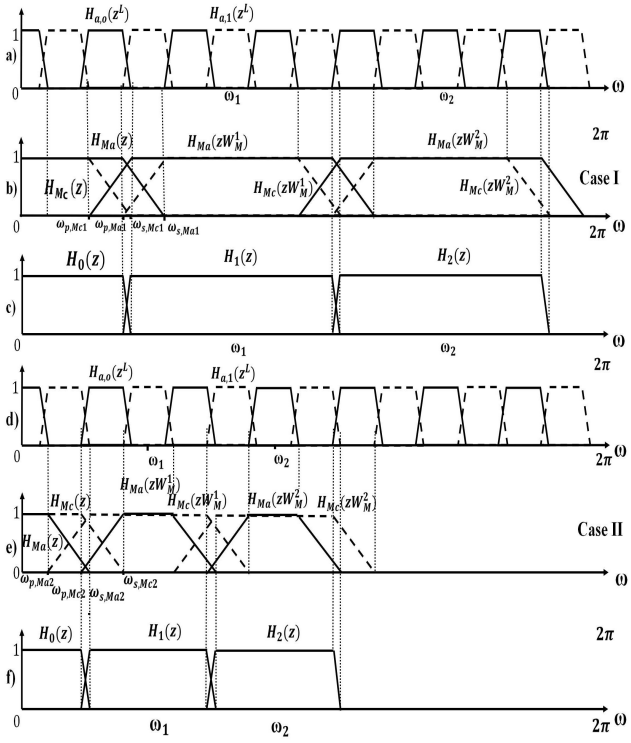

Fig. 5. Design principle of the proposed alternate masking scheme

The complexity of the modal filter, DFT unit, and the two masking filters includes the number of multipliers used for the prototype filter's design, μ_{pr}. Mathematically,

$$\mu_{pr} = \mu_{modal} + (m+1)log_2(m+1) + \mu_{ma,modal} + \mu_{ma,is} + \mu_{mc,modal} + \mu_{mc,is} \quad (12)$$

where μ_{modal} is the number of multipliers required for modal filter design, $\mu_{ma,modal}$ and $\mu_{ma,is}$ denote the multipliers of the IFIR modal filter, and image-suppressor filter for the masking filter, $H_{Ma}(z)$. Likewise, $\mu_{mc,modal}$ and

$\mu_{mc,is}$ denote the multipliers of the IFIR modal filter and image-suppressor filter for the masking filter, $H_{Mc}(z)$. The complexity of the DFT unit is specified by $(m+1)log_2(m+1)$ which is meagre (19**?**). Thus, the lower-order modal filter and masking filters implemented using IFIR technique will result in overall lesser number of multipliers for the design of ModFRM prototype filter.

In the second phase, an innovative masking scheme is introduced to generate the M-channel analysis filter bank by alternately masking the remaining spectra replicas in the even BES and odd BES filters with the appropriately modulated masking filters. By invoking (5), the analysis filters $H_k(z)$, can be expressed as:

$$H_k(z) = \sum_{i=0}^{p} H_{a,2i}(z^L)H_{Ma}(zW_M^k)+ \sum_{i=0}^{p} H_{a,2i+1}(z^L)H_{Mc}(zW_M^k) \quad ;for \;\; k \;\; even \tag{13}$$

$$H_k(z) = \sum_{i=0}^{p} H_{a,2i}(z^L)H_{Mc}(zW_M^k)+ \sum_{i=0}^{p} H_{a,2i+1}(z^L)H_{Ma}(zW_M^k) \quad ;for \;\; k \;\; odd \tag{14}$$

where $W_M = e^{-j\frac{2\pi}{M}}$ and $k = 0, 1, ...M-1$. Also,

- $\sum_{i=0}^{p} H_{a,2i}(z^L)$ represents the even BES-FB
- $\sum_{i=0}^{p} H_{a,2i+1}(z^L)$ represents the odd BES-FB.

Figure 5 demonstrates the proposed AMS. The number of modulated filters is set to $m = 1$ to simplify the analysis. As in Figure 5a, for $m = 1$, $H_{a,0}(z^L)$ and $H_{a,1}(z^L)$ represent the BES-FBs. The channel $H_0(z)$ in Figure 5c is obtained by masking $H_{a,0}(z^L)$ and $H_{a,1}(z^L)$ with $H_{Ma}(z)$ and $H_{Mc}(z)$. For $H_1(z)$, $H_{a,0}(z^L)$ should be masked with $H_{Mc}(zW_M^1)$ instead of $H_{Ma}(zW_M^1)$. Case II, depicted in Figure 5e and Figure 5f, is likewise designed.

The number of multipliers of ModFRM prototype filter (μ_{pr}) and two DFT transition blocks for the masking filters constitutes for the complete multiplier complexity of the M-channel ModFRM-FB. Mathematically, it is represented as:

$$\mu_{ModFRMFB} = \mu_{pr} + 2Mlog_2M \tag{15}$$

This method of alternately masking the spectral replicas in even BES-FB and odd BES-FB to generate multiple channels using the same set of masking filters is very new, and it accounts for the significant reduction in hardware. However, as with the traditional FRM technique, the reduced complexity of ModFRM architecture comes at the cost of a longer delay, which is dominantly contributed by the delay of the masking filter pair used for the AMS.

The overall delay D can be calculated as:

$$D = L \times D_a + D_{mask} \tag{16}$$

where D_a is the delay of the modal filter and D_{mask} is the delay of the two masking filters. Since masking filters can differ in length, the delay provided by each masking filter will also differ. Hence, to avoid phase distortion, the length of the masking filters must be equalized.

$$D_{mask} = max(D_{Ma}, D_{Mc}) \tag{17}$$

where D_{Ma} is the delay of $H_{Ma}(z)$ and D_{Mc} is the delay of $H_{Mc}(z)$. As D_a must be an integer, $D - D_{mask}$ must be a multiple of L. Therefore, additional delays must be added to D_{mask} in order to satisfy this criterion.

III. Proposed Design of Multiplier-Less ModFRM-FB

In the proposed method, the ModFRM's sub-filter coefficients are approximated to the smallest number of SOPOT terms by applying the MPGBP algorithm (20).

Let $h(n)$ be a filter of order $N-1$.

$$h = [h(0)\ h(1)\ \cdots h(N-1)]^T \tag{18}$$

A Dictionary $D = [\pm d_1, \pm d_2, \cdots \pm d_Q]$ is constructed, with $\pm d_j \in R^N$ being a vector of N components, P being the number of nonzero components of magnitude one and $(N–P)$ being zero. Vector d_i are permutations of the form:

$$d_j = [\pm 1^P 0^{(N-P)}]^T := [\underbrace{\pm 1 \ldots \pm 1}_{P \text{ times}} \ \underbrace{00\ldots00}_{(N-P) \text{ times}}]^T. \tag{19}$$

As defined in Algorithm 1, these vectors are used to successively approximate the coefficients in h.

After K steps, the MPGBP algorithm returns a SOPOT approximation (SA) of h, presented as:

$$h^{(K)}(n) = \sum_{k=1}^{K} 2^{-p_k} d_{j_k}(n), \quad \text{for } n \in [0, N-1]. \tag{20}$$

Algorithm 1: MPGBP Algorithm

1 Start with $k = 1$, $r_1 = h$.
2 Repeat until you reach the following stop criterion:
(a) Locate the most closely related code-word, i.e. locate $j_k \in \{1, \cdots Q\}$ such that

$$\langle r_k, d_{j_k} \rangle = \max_{1 \le j \le Q} \{|\langle r_k, d_j \rangle|\} \tag{21}$$

(b) Select

$$p_k = \left\lceil \log_{\frac{1}{2}} \left(\frac{4\langle r_k, d_{j_k} \rangle}{3} \right) \right\rceil \tag{22}$$

(c) Replace

$$r_{k+1} \leftarrow r_k - (2)^{-p_k} d_{j_k} \tag{23}$$

(d) Increment k.
3 Stop

As the code-vectors are permutations of -1, 1, or 0, finding the inner product $\langle r_k, d_{j_k} \rangle$ is similar to adding the coordinates

of r_k corresponding to the coordinates of d_{j_k} equal to 1 and deducting the coordinates of r_k corresponding to the coordinates of d_{j_k} equal to -1. Therefore two conditions must be met to obtain the greatest inner product:

(I) The sign of the respective coordinates of r_k of d_{j_k} has to be the same.

(II) Largest magnitude coordinates should be 1 or -1.

Algorithm 2: MPGBP: Fast Algorithm

1 Sort the absolute values of the coordinates of updated residue, r in decreasing order of magnitude, and save the indexes of the P greatest ones.

2 Set the indices of the P coordinates that were saved in step 1 to +1 when the coordinate is positive and -1 when the coordinate is negative. The rest of the coordinates are set to zero.

With this understanding, Algorithm 2 (20) describes a fast algorithm for locating the nearest vector r_m to a vector d_{j_k}. The MPGBP design is repeated with dictionaries of various P values from 1 to $\left\lfloor \sqrt{N_{min}(1+\gamma)/2} \right\rfloor$ for various N from N_{min} to $\lceil N_{min}(1+\gamma) \rceil$ to achieve optimal SOPOT approximations. Here $\gamma < 1$, specifies the range of filter lengths to be tried and N_{min} is the minimum order of the filter designed using the Parks–McClellan algorithm. Among all these designs, the design with lowest the number of SOPOTs, while satisfying the given specifications is chosen. The design time of the proposed system is calculated as the time required for designing the subfilters for the ModFRM prototype filter, MPGBP iterations (for different values of N and P) for these filters, and filter response evaluation for each of the MPGBP iteration to attain filters that meet the specified specifications.

To further reduce the hardware cost, the MPGBP algorithm's output is subjected to a post-processing operation known as common-subexpression elimination (CSE) to share the redundant POT words across the coefficients. Finally, the number of common subexpressions, as well as the number of spare POT words decides the hardware cost.

IV. Result Analysis

To begin, the hardware efficiency of the ModFRM approach in terms of the total number of multiplications per input sample (mults/sample) is calculated and is compared with direct realization and classic FRM techniques in Table I. For the computation, the knowledge that interpolation reduces the number of mults/sample of a filter of length $(N+1)$ to $\frac{(N+1)}{L}$ as well as the coefficient symmetry attribute of the linear phase FIR filter is used (**?**).

The prototype filter specifications selected for the analysis are passband edge frequency of 0.06π, stopband edge frequency of 0.065π, passband ripple of 0.0065dB, and stopband attenuation of 60dB. The frequency specifications of the FRM and ModFRM subfilters to meet the desired specifications are provided in Table I. It is inferred from Table I that the ModFRM structure's modal filter has more relaxed specifications than the modal filter used in the conventional FRM structure for a given prototype filter design. As the filter order is inversely related to the transition-width (1), the complexity of constructing the modal filter of the ModFRM structure will be substantially lesser than that of the FRM architecture. However, the wider transition width of ModFRM modal filter will necessitate a larger L value to build the desired filter specification. As a result, L = 20, which is two times the interpolation factor used in the conventional FRM technique, is used in this method. Similarly, the masking filters of the ModFRM structure designed using the IFIR technique with $L_{IFIR} = 6$ show a significant reduction in complexity in contrast to the masking filters of conventional FRM structure. This results in an overall lower complexity of the ModFRM prototype filter. In the next step, using the novel AMS, a 16-channel ModFRM-FB is generated. With the AMS, the spectral replicas resulting from the interpolation is efficiently utilized for constructing multiple channels, with the same set of masking filters. On the other hand, to construct each channel, a conventional FRM structure will need a distinct set of band-pass masking filters resulting in a very high computational load.

The performance and hardware complexity of the ModFRM-FB is compared with some recently introduced FBs in Table II and Table III respectively. The results show a drastic reduction in hardware complexity with better performance for the proposed ModFRM-FB using AMS.

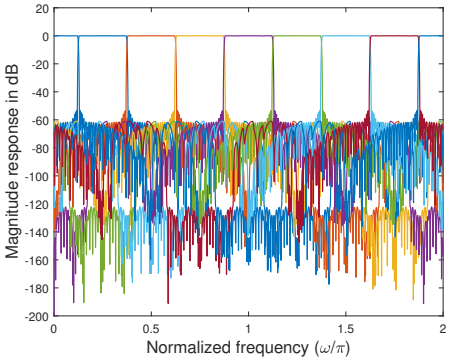

Fig. 6. Uniform 8 channel ModFRM-FB

Now, to demonstrate the hardware efficiency of the proposed ModFRM using MPGBP algorithm in SDR channelizers, we have considered the design example in (14) that handle 4 wireless CDMA2000 standards. A continuous coefficient 8-channel ModFRM-FB is initially designed for this. The passband frequency and stopband frequency of the modal filter is considered as 0.2π and 0.3π. As per Equation (4), m is calculated as 3. The filter specifications for the masking filters are calculated using (6) and is given in Table IV. Subsequently, using Equations (8) to (11), the specifications of IFIR modal filter and the image-suppressor filter for the masking filters are determined for the optimum interpolation factor, L_{IFIR} and are given in Table V and VI. While designing, note that passband ripple of the IFIR sub-filters is chosen as half that of the desired passband ripple (18).

TABLE I
COMPARISON OF COMPUTATIONAL COMPLEXITY BASED ON MULTIPLICATIONS PER INPUT SAMPLE

Method	Subfilter	Passband edge frequency	Stopband edge frequency	Filter Order	Mults/sample
Direct FIR		0.06π	0.065π	1348	675
Conventional FRM	1. Modal filter, $H_a(z)$	0.35π	0.4π	67	98.4
	2. Masking filter, $H_{Ma}(z)$	0.04π	0.065π	142	
	3. Masking filter, $H_{Mc}(z)$	0.06π	0.135π	44	
Proposed ModFRM	1. Modal filter, $H_a(z)$	0.2π	0.3π	63	53.266
	2. IFIR modal filter for $H_{Ma}(z)$	0.36π	0.51π	52	
	3. IFIR image-suppressor filter for $H_{Ma}(z)$	0.06π	0.248π	40	
	4. IFIR modal filter for $H_{Mc}(z)$	0.24π	0.39π	52	
	5. IFIR image-suppressor filter for $H_{Mc}(z)$	0.04π	0.268π	30	

TABLE II
PERFORMANCE COMPARISON WITH DIFFERENT FB APPROACHES

Method	No. of channels (*M*)	Transition width	Passband ripple (dB)	Stop band attenuation (dB)	Amplitude distortion
CMFB (19; 21)	8	0.01	0.004	60.07	0.018
MDFT (19; 22)	8	0.01	0.004	60	0.043
Proposed ModFRM	8	0.01	0.0065	60	0.018
CMFB (19; 21)	32	0.0025	0.004	60.07	0.0041
MDFT (19; 22)	32	0.0025	0.004	61.9	0.089
Proposed ModFRM	32	0.0025	0.0065	60	0.023

TABLE III
HARDWARE COMPLEXITY COMPARISON WITH DIFFERENT FB APPROACHES

Method	No. of channels (*M*)	No. of multipliers of the prototype filter	Complexity of modulation block	Total Multipliers
CMFB (19; 21)	8	698	$\frac{8}{2}log_2 8$+8	718
MDFT (19; 22)	8	174	$8log_2 8$+8	206
Proposed ModFRM	8	106	$8log_2 8 + 8log_2 8$	154
CMFB (19; 21)	32	1396	$\frac{32}{2}log_2 32$+32	1588
MDFT (19; 22)	32	720	$32log_2 32$+32	912
Proposed ModFRM	32	145	$32log_2 32 + 32log_2 32$	465

TABLE IV
FREQUENCY SPECIFICATION FOR THE MASKING FILTERS OF 8-CHANNEL MODFRM-FB

Interpolation factor	$H_{Ma}(z)$		$H_{Mc}(z)$		ModFRM prototype filter	
	Pb	Sb	Pb	Sb	Pb	Sb
10	0.12π	0.17π	0.08π	0.13π	0.12π	0.13π

TABLE V
FREQUENCY SPECIFICATION OF THE SUBFILTERS IN THE IFIR IMPLEMENTATION OF $H_{Ma}(z)$

L_{IFIR}	IFIR modal filter		Image-suppressor filter	
	Pb	Sb	Pb	Sb
3	0.36π	0.51π	0.12π	0.4967π

TABLE VI
FREQUENCY SPECIFICATION OF THE SUBFILTERS IN THE IFIR IMPLEMENTATION OF $H_{Mc}(z)$

l_{IFIR}	IFIR modal filter		Image-suppressor filter	
	Pb	Sb	Pb	Sb
3	0.24π	0.39π	0.08π	0.5367π

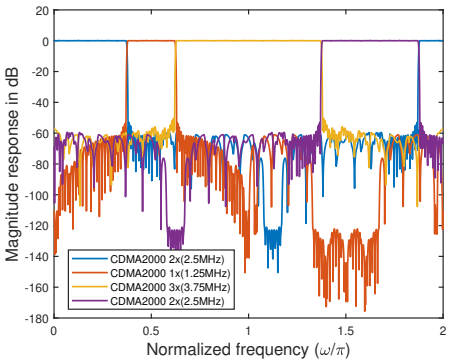

Fig. 7. Four wireless CDMA2000 standards accomplished by merging adjacent channels of uniform 8-channel ModFRM-FB

The uniform 8-channel designed using ModFRM architecture using the AMS is given in Figure 6. The four wireless CDMA2000 standards accomplished by merging adjacent channels with channel allocation (c_0,c_1,c_2,c_3)=(2,1,3,2) is shown in Figure 7.

The continuous coefficient FB is then converted to SOPOT terms using the MPGBP algorithm. The procedure is repeated for different values of N and P. Table [VII]-[XI] display the best results for sub-filter designs with varying P and N in terms of the number of adders. The number of adders and POT terms desired for a multiplier-less realization, Normalized Peak Ripple (NPR), Normalized Frequency Response Error (NFRE), and the time required to build the SOPOT filters when simulated with MATLAB R2020a running on a Windows 10

TABLE VII
DESIGN METRICS OF MODAL FILTER, $H_a(z)$.

No. of Adders	N	P	No. of POTs	Normalized Peak Ripple(dB)	Normalized Frequency Response Error	Design Time(sec)
96	76	1	13	60.502521	0.000472	0.016042
96	78	1	13	61.122380	0.000515	0.026173
97	76	2	13	61.447365	0.00436	0.022970
97	78	2	13	60.741821	0.0005	0.009291
98	76	3	13	61.754349	0.000425	0.023016
98	78	3	13	61.310370	0.000471	0.010173
98	90	3	13	60.104123	0.000730	0.009865
99	78	4	13	61.611161	0.000432	0.008660
96	78	5	13	61.122380	0.00515	0.006975
102	76	6	13	61.618476	0.000363	0.005404

TABLE VIII
DESIGN METRICS OF IFIR MODAL FILTER FOR $H_{Ma}(z)$

No. of Adders	N	P	No. of POTs	Normalized Peak Ripple(dB)	Normalized Frequency Response Error	Design Time(sec)
76	58	1	13	60.858011	0.000299	0.006688
79	56	2	13	60.806615	0.000289	0.005956
77	56	3	13	60.292693	0.000326	0.004700
79	58	4	13	61.524763	0.000268	0.004184
80	56	5	13	61.286372	0.000281	0.003334

TABLE IX
DESIGN METRICS OF IFIR IMAGE-SUPPRESSOR FILTER FOR $H_{Ma}(z)$

No. of Adders	N	P	No. of POTs	Normalized Peak Ripple(dB)	Normalized Frequency Response Error	Design Time(sec)
29	17	1	11	60.417800	0.000307	0.002901
30	19	2	11	60.685813	0.000345	0.002182
31	18	1	13	61.055678	0.000165	0.006013
32	19	1	12	60.975549	0.000222	0.005552
32	18	2	13	60.447350	0.000159	0.002598
32	20	2	12	61.295812	0.000336	0.002403
33	20	1	13	60.993974	0.000261	0.004167
34	18	3	14	61.031193	0.000102	0.001750
35	23	1	10	61.487269	0.000581	0.003838

TABLE X
DESIGN METRICS OF IFIR MODAL FILTER FOR $H_{Mc}(z)$

No. of Adders	N	P	No. of POTs	Normalized Peak Ripple(dB)	Normalized Frequency Response Error	Design Time(sec)
71	61	1	12	60.946354	0.000461	0.007724
73	61	2	12	61.468379	0.000416	0.004979
76	61	5	12	61.333199	0.000372	0.004461
78	55	3	12	62.652428	0.000235	0.004324
79	70	4	12	61.956879	0.000577	0.003916
80	53	3	12	61.615098	0.000255	0.003488
80	70	3	12	60.605269	0.000573	0.005398

TABLE XI
DESIGN METRICS OF IFIR IMAGE-SUPPRESSOR FILTER FOR $H_{Mc}(z)$

No. of Adders	N	P	No. of POTs	Normalized Peak Ripple(dB)	Normalized Frequency Response Error	Design Time(sec)
22	16	1	10	60.240054	0.000556	0.002356
23	17	2	10	60.751750	0.000520	0.001806
25	20	1	11	61.748855	0.001305	0.002801
26	20	3	11	61.774638	0.000865	0.001693
29	21	1	10	61.059140	0.000936	0.002985
31	21	2	10	62.211553	0.000593	0.002262

64-bit operating system on an Intel(R) Core(TM) i5-7200U CPU 2.5GHz, are all specified in Table [VII]-[XI]. We have measured NPR and NFRE as in (23) to compare the performance of the constructed filters. Among the results, the designs that have low complexity and better ripple specifications are identified as the appropriate one. The impulse response of these selected subfilters are presented in Tables [XII]-[XVI]. Note that it is enough to apply the MPGBP method to only half the filter coefficients as the coefficients are symmetric. The magnitude responses of MPGBP design of the ModFRM subfilters are plotted in Figure [8]-[12]. The ModFRM prototype filter and the SA design are depicted in Figure 13. The overall

TABLE XII
SA COEFFICIENTS OF $H_a(z)$ $(P=1, N=76, h(76-n)=h(n)$ FOR $n=0,1,...38)$.

n	h(n)	POTs	n	h(n)	POTs
0	-0.0003662109375	$-2^{-11}+2^{-13}$	20	0.009765625	$2^{-7}+2^{-9}$
1	-0.000244140625	-2^{-12}	21	0.00811767578125	$2^{-7}+2^{-12}+2^{-14}$
2	0	0	22	0.00048828125	2^{-11}
3	0.00042724609375	$2^{-11}-2^{-14}$	23	-0.00970458984375	$-2^{-7}-2^{-9}+2^{-14}$
4	0.000732421875	$2^{-10}-2^{-12}$	24	-0.0159912109375	$-2^{-6}-2^{-11}+2^{-13}$
5	0.000732421875	$2^{-10}-2^{-12}$	25	-0.01318359375	$-2^{-6}+2^{-9}-2^{-11}$
6	0.0001220703125	2^{-13}	26	-0.00048828125	-2^{-11}
7	-0.0009765625	-2^{-10}	27	0.01611328125	$2^{-6}+2^{-11}$
8	-0.001708984375	$-2^{-9}+2^{-12}$	28	0.0267333984375	$2^{-5}-2^{-8}+2^{-11}+2^{-13}$
9	-0.001525878906250	$-2^{-9}+2^{-11}+2^{-14}$	29	0.0220947265625	$2^{-6}+2^{-7}-2^{-10}+2^{-11}-2^{-13}$
10	-0.0001220703125	-2^{-13}	30	0.0006103515625	$2^{-11}+2^{-13}$
11	0.00189208984375	$2^{-9}-2^{-14}$	31	-0.029052734375	$-2^{-5}+2^{-9}-2^{-12}$
12	0.0032958984375	$2^{-8}-2^{-11}+2^{-13}$	32	-0.0498046875	$-2^{-4}+2^{-6}+2^{-8}+2^{-10}$
13	0.0029296875	$2^{-8}-2^{-10}$	33	-0.04351806640625	$-2^{-5}-2^{-6}+2^{-8}+2^{-11}-2^{-14}$
14	0.000244140625	2^{-12}	34	-0.0006103515625	$-2^{-11}-2^{-13}$
15	-0.00341796875	$-2^{-8}+2^{-11}$	35	0.0733642578125	$2^{-4}+2^{-7}+2^{-8}-2^{-10}-2^{-13}$
16	-0.005859375	$-2^{-7}+2^{-9}$	36	0.1580810546875	$2^{-3}+2^{-5}+2^{-9}-2^{-13}$
17	-0.004943844765625	$-2^{-8}-2^{-10}-2^{-14}$	37	0.22509765625	$2^{-2}-2^{-5}-2^{-7}-2^{-9}-2^{-11}$
18	-0.00030517578125	$-2^{-12}+2^{-14}$	38	0.2506103515625	$2^{-2}+2^{-11}+2^{-13}$
19	0.005859375	$2^{-7}-2^{-9}$			

stopband attenuation of ModFRM prototype filter constructed with the MPGBP algorithm is 60.74dB, which is pretty close to that of the continuous ModFRM prototype filter (61.48dB). Thus, in the design of the overall ModFRM prototype filter, the slight changes in the frequency response of the sub-filters on approximating are found to compensate for each other. Hence, from the design point of view, the proposal is very effective as it allows estimating the filter coefficients with the number of adders close to the filter order while attaining the prescribed specifications.

TABLE XIII
SA COEFFICIENTS OF IFIR MODAL FILTER FOR $H_{Ma}(z)$ $(P=1, N=58, h(58-n)=h(n)$ FOR $n=0,1,...29)$.

n	h(n)	POTs	n	h(n)	POTs
0	0	0	15	0.00445556640625	$2^{-8}+2^{-11}+2^{-14}$
1	0.000244140625	2^{-12}	16	-0.01068115234375	$-2^{-7}-2^{-8}+2^{-10}-2^{-14}$
2	-0.0001220703125	-2^{-13}	17	-0.01123046875	$-2^{-6}+2^{-8}-2^{-11}$
3	-0.00054931640625	$-2^{-11}-2^{-14}$	18	0.01000976562 5	$2^{-7}+2^{-9}+2^{-12}$
4	0.00006103515625	2^{-14}	19	0.0205078125	$2^{-6}+2^{-8}+2^{-10}$
5	0.0010986328125	$2^{-10}+2^{-13}$	20	-0.0047607421875	$-2^{-8}-2^{-10}+2^{-13}$
6	0.00042724609375	$2^{-11}-2^{-14}$	21	-0.03155517578125	$-2^{-5}-2^{-12}-2^{-14}$
7	-0.001708984375	$-2^{-9}+2^{-12}$	22	-0.0078125	-2^{-7}
8	-0.001525878906250	$-2^{-9}+2^{-11}+2^{-14}$	23	0.04290771484375	$2^{-5}+2^{-6}-2^{-8}+2^{-14}$
9	0.0020751953125	$2^{-9}+2^{-13}$	24	0.03271484375	$2^{-5}+2^{-9}-2^{-11}$
10	0.00341796875	$2^{-8}-2^{-11}$	25	-0.0528564453125	$-2^{-4}+2^{-7}-2^{-9}+2^{-13}$
11	-0.001708984375	$-2^{-9}+2^{-12}$	26	-0.085693359375	$-2^{-4}-2^{-5}+2^{-7}-2^{-12}$
12	-0.006103515625	$-2^{-7}+2^{-9}+2^{-12}$	27	0.05963134765625	$2^{-4}-2^{-8}-2^{-10}+2^{-14}$
13	-0.000244140625	-2^{-12}	28	0.3111572265625	$2^{-2}+2^{-4}-2^{-10}+2^{-11}-2^{-13}$
14	0.0087890625	$2^{-7}+2^{-10}$	29	0.43798828125	$2^{-1}-2^{-4}-2^{-11}$

TABLE XIV
SA COEFFICIENTS OF IFIR IMAGE-SUPPRESSOR FILTER FOR $H_{Ma}(z)$ $(P=1, N=17, h(17-n)=h(n)$ FOR $n=0,1,...8)$

n	h(n)	POTs	n	h(n)	POTs
0	0.003298984375	$2^{-8}-2^{-11}+2^{-13}$	5	-0.019775390625	$-2^{-6}-2^{-8}-2^{-12}$
1	0.0069580078125	$2^{-7}-2^{-10}-2^{-13}$	6	0.06787109375	$2^{-4}+2^{-8}+^{-9}-2^{-11}$
2	0.001708984375	$2^{-9}-2^{-12}$	7	0.19921875	$2^{-2}-2^{-4}-2^{-6}-2^{-8}$
3	-0.01904296875	$-2^{-6}-2^{-8}+2^{-11}$	8	0.298828125	$2^{-2}+2^{-4}-2^{-6}-2^{-9}$
4	-0.039306640625	$2^{-5}-2^{-7}-2^{-12}$			

The adder cost is further reduced using the common sub-expression elimination (CSE) algorithm (16; 17). The total number of adders in the proposed multiplier-less implementation of the ModFRM is now calculated by combining structural adders and POT terms adders after considering the various common sub-expressions amongst the coefficients. The hardware complexity before and after using the MPGBP and CSE is compared in Table XVII. For the chosen example, the design time is calculated to be $15.1325s$.

From Table III, it has been inferred that MDFT-FB has a complexity that is comparable to the proposed ModFRM-

TABLE XV
SA COEFFICIENTS OF IFIR MODAL FILTER FOR $H_{Mc}(z)$ $(P = 1, N = 61, h(61-n) = h(n)$ FOR $n = 0, 1, ...30)$.

n	h(n)	POTs	n	h(n)	POTs
0	0.000000000000	0	16	0.009765625	$2^{-7}+2^{-9}$
1	-0.000244140625	-2^{-12}	17	0.009765625	$2^{-7}+2^{-9}$
2	0.000000000000	0	18	-0.001220703125	$-2^{-10}-2^{-12}$
3	0.000244140625	2^{-12}	19	-0.01538085937	$-2^{-6}+2^{-12}$
4	0.0006103515625	$2^{-11}+2^{-13}$	20	-0.01806640625	$-2^{-6}-2^{-9}-2^{-11}$
5	0.000305175781250	$2^{-12}+2^{-14}$	21	-0.00146484375	$-2^{-9}+2^{-11}$
6	-0.0006103515625	$-2^{-11}-2^{-13}$	22	0.0235595703125	$2^{-5}-2^{-7}-2^{-13}$
7	-0.00146484375	$-2^{-9}+2^{-11}$	23	0.03271484375	$2^{-5}+2^{-9}-2^{-11}$
8	-0.0009765625	-2^{-10}	24	0.0086669921875	$2^{-7}+2^{-10}-2^{-13}$
9	0.001220703125	$2^{-10}+2^{-12}$	25	-0.0372314453125	$-2^{-5}-2^{-7}+2^{-9}+2^{-13}$
10	0.003173828125	$2^{-8}-2^{-10}-2^{-12}$	26	-0.064453125	$-2^{-4}-2^{-9}$
11	0.002380371093 7	$2^{-9}+2^{-11}-2^{-14}$	27	-0.030029296875	$-2^{-5}+2^{-10}-2^{-12}$
12	-0.001708984375	$-2^{-9}+2^{-12}$	28	0.07507324218 75	$2^{-4}+2^{-6}-2^{-8}-2^{-10}-2^{-13}$
13	-0.00585937 5	$-2^{-7}+2^{-9}$	29	0.2099609375	$2^{-2}-2^{-5}+2^{-7}+2^{-10}$
14	-0.005004882812 5	$-2^{-8}-2^{-10}-2^{-13}$	30	0.304443359375	$2^{-2}+2^{-4}-2^{-7}+2^{-12}$
15	0.001953125	2^{-9}			

TABLE XVI
SA COEFFICIENTS OF IFIR IMAGE-SUPPRESSOR FILTER FOR $H_{Mc}(z)$ $(P = 1, N = 16, h(16-n) = h(n)$ FOR $n = 0, 1, ...8)$

n	h(n)	POTs	n	h(n)	POTs
0	0.00244140625	$2^{-9}+2^{-11}$	5	0.0087890625	$2^{-7}+2^{-10}$
1	0.0048828125	$2^{-8}+2^{-10}$	6	0.125	2^{-3}
2	-0.00244140625	$-2^{-9}-2^{-11}$	7	0.260009765625	$2^{-2}+2^{-7}+2^{-9}+2^{-12}$
3	-0.02392578125	$-2^{-5}+2^{-7}+2^{-11}$	8	0.32080078125	$2^{-2}+2^{-4}+2^{-7}+2^{-11}$
4	-0.03515625	$-2^{-5}-2^{-8}$			

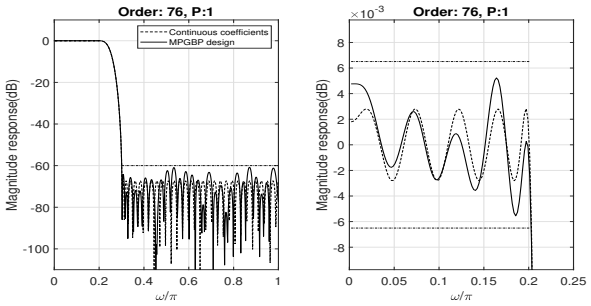

Fig. 8. Frequency response of the modal filter and its SA design $(N = 76$ and $P = 1)$

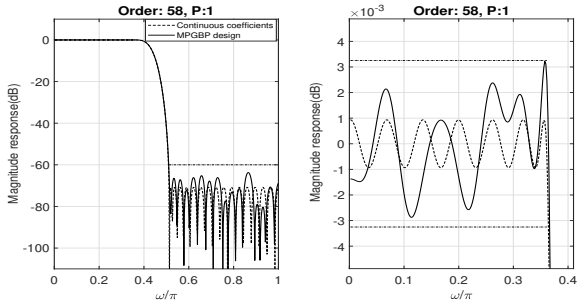

Fig. 9. Frequency response of the IFIR modal filter for $H_{Ma}(z)$ and its SA design $(N = 58$ and $P = 1)$

FB. Hence performance comparison of the proposed ModFRM multiplier-less approach is done with the multiplier-less MDFT-FB attained through various metaheuristic algorithms in Table XVIII. Table XIX compares the proposed ModFRM-FB employing MPGBP to various optimization algorithms in terms of hardware complexity and run time. The results show that the proposed multiplier-less design has lower hardware complexity and run-time than existing methods.

Just as it was to the CDMA standard in this study, it may be applied to a variety of other standards as well. However, this would have little effect on the overall trend of the results, making it more suitable for SDR channelizers.

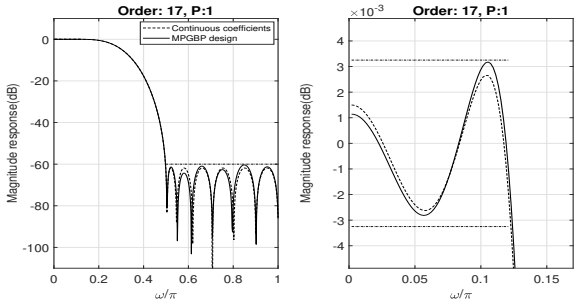

Fig. 10. Frequency response of IFIR image-suppressor filter for $H_{Ma}(z)$ and its SA design $(N = 17$ and $P = 1)$.

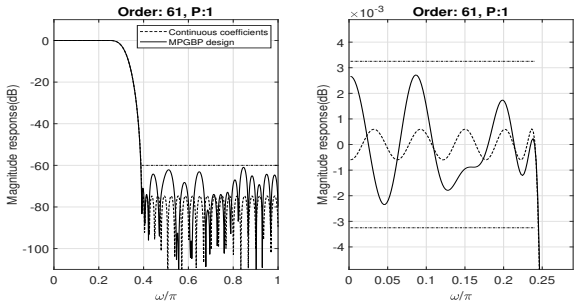

Fig. 11. Frequency response of IFIR modal filter for $H_{Mc}(z)$ and its SA design $(N = 61$ and $P = 1)$.

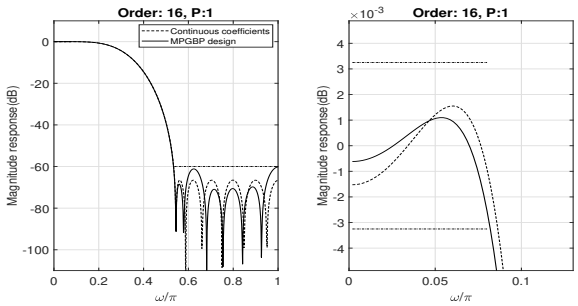

Fig. 12. Frequency response of IFIR image-suppressor filter for $H_{Mc}(z)$ and its SA design $(N = 17$ and $P = 1)$

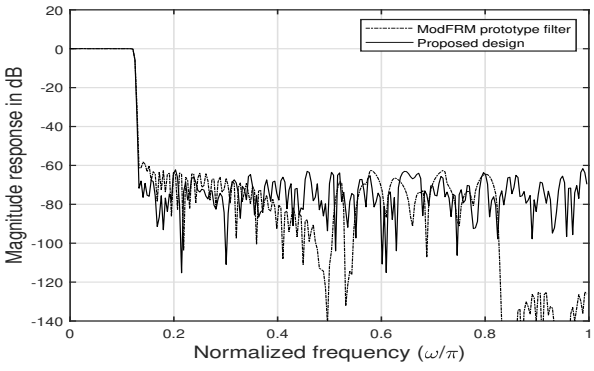

Fig. 13. Frequency responses of ModFRM prototype filter and its SA design

TABLE XVII
HARDWARE COMPLEXITY COMPARISON AFTER EACH STAGE

	Multipliers	Coefficient Adders	Structural Adders	Total Adders
Modal filter, $H_a(z)$				
-With continuous coefficients	32	0	64	64
-After MPGBP approximation	0	58	76	134
-After CSE	0	26	76	102
IFIR modal filter for $H_{Ma}(z)$				
-With continuous coefficients	25	0	49	49
-After MPGBP approximation	0	47	58	105
-After CSE	0	25	58	83
IFIR image-suppressor filter for $H_{Ma}(z)$				
-With continuous coefficients	9	0	17	17
-After MPGBP approximation	0	20	17	37
-After CSE	0	13	17	30
IFIR modal filter for $H_{Mc}(z)$				
-With continuous coefficients	24	0	48	48
-After MPGBP approximation	0	42	61	103
-After CSE	0	20	61	81
IFIR image-suppressor filter for $H_{Mc}(z)$				
-With continuous coefficients	8	0	16	16
-After MPGBP approximation	0	13	16	29
-After CSE	0	7	16	23

TABLE XVIII
PERFORMANCE COMPARISON OF THE PROPOSED MODFRM-FB USING MPGBP WITH OTHER OPTIMIZATION ALGORITHMS

Architecture	Algorithm	Passband ripple	Stopband attenuation	Transition width	Amplitude distortion of filter bank
MDFT-FB (24)	Continuous coefficients	0.0083	62.92	0.003	0.02296
	16 bits	0.00798	62.9	0.003	0.02724
	Maximum precision(7 SPT)	0.01103	59.81	0.003	0.02359
	CSD rounded (3 SPT)	0.07075	41.81	0.003	0.1408
	Integer coded GA	0.02166	50.08	0.003	0.03901
	Integer coded DE	0.01728	51.6	0.003	0.03464
	Integer coded ABC	0.01138	53.55	0.003	0.02298
	Integer coded HSA	0.00988	55.29	0.003	0.0198
	Integer coded GSA	0.00817	58.32	0.003	0.01634
Proposed ModFRM-FB	MPGBP	0.006576	61.501	0.003	0.023

TABLE XIX
PERFORMANCE COMPARISON OF THE PROPOSED MODFRM-FB USING MPGBP WITH OTHER OPTIMIZATION ALGORITHMS

Architecture	Algorithm	No. of multipliers	No. of POT adders	Design time (sec)
MDFT-FB (24)	Continuous coefficients	198	-	-
	16 bits	0	467	-
	Maximum precision (7 SPT)	0	344	-
	CSD rounded (3 SPT)	0	287	-
	Integer coded GA	0	326	1140.82
	Integer coded DE	0	313	591.70
	Integer coded ABC	0	300	1145.98
	Integer coded HSA	0	300	738.59
	Integer coded GSA	0	300	701.51
Proposed ModFRM-FB	MPGBP	0	150	15.1325

V. CONCLUSION

In this paper, a hardware-efficient SDR channelizer is proposed. For this, the layout of the well-known FRM technique is redesigned by replacing the modal and complementary filters in the upper and lower branches with two power-complementary and linear phase filter banks. A novel masking technique is also adopted for generating uniform filter banks to guarantee the full utilization of the spectra. Finally, by combining the adjoining uniform channels, non-uniform channels for extracting different communication standards in the software-defined radio channelizer are created. The proposed system is made multiplier-less by approximating the continuous coefficients using a dictionary of vectors to give an optimal sum-of-power-of-two representation. Results show that the proposed multiplier-less design has lower complexity than existing methods, making it a better option for channel filters in SDR receivers. Furthermore, in contrast to all other general optimization methods, the proposed approach is much faster because it needs no initial parameter configuration or exhaustive search schemes.

REFERENCES

[1] Y. Lim, "Frequency-response masking approach for the synthesis of sharp linear phase digital filters," *IEEE transactions on circuits and systems*, vol. 33, no. 4, pp. 357–364, 1986. [Online]. Available: https://doi.org/10.1109/TCS.1986.1085930

[2] M. B. Furtado, P. S. Diniz, and S. L. Netto, "Optimized prototype filter based on the FRM approach for cosine-modulated filter banks," *Circuits, Systems and Signal Processing*, vol. 22, no. 2, pp. 193–210, 2003. [Online]. Available: https://doi.org/10.1007/s00034-004-7026-0

[3] M. Furtado, P. S. Diniz, S. L. Netto, and T. Saramaki, "On the design of high-complexity cosine-modulated transmultiplexers based on the frequency-response masking approach," *IEEE Transactions on Circuits and Systems I: Regular Papers*, vol. 52, no. 11, pp. 2413–2426, 2005. [Online]. Available: https://doi.org/10.1109/TCSI.2005.853919

[4] N. Li and B. Nowrouzian, "Application of frequency-response masking technique to the design of a novel modified-DFT filter bank," in *2006 IEEE International Symposium on Circuits and Systems*. IEEE, 2006, pp. 4–pp. [Online]. Available: https://doi.org/10.1016/j.engappai.2012.02.010

[5] T. Chen, P. Li, W. Zhang, and Y. Liu, "A novel channelized FB architecture with narrow transition bandwidth based on CEM FRM," *Annals of Telecommunications*, vol. 71, no. 1-2, pp. 27–33, 2016. [Online]. Available: https://doi.org/10.1007/s12243-015-0477-4

[6] W. Zhang, Q. Du, Q. Ji, and T. Chen, "Unified FRM-based complex modulated filter bank structure with low complexity," *Electronics Letters*, vol. 54, no. 1, pp. 18–20, 2017. [Online]. Available: https://doi.org/10.1049/el.2017.3244

[7] Y. Lian and Y. J. Yu, "Guest editorial: Low-power digital filter design techniques and their applications," *Circuits, Systems, and Signal Processing*, vol. 29, no. 1, p. 1, 2010. [Online]. Available: https://doi.org/10.1007/s00034-009-9110-y

[8] V. Sakthivel and E. Elias, "Design of low complexity sharp MDFT filter banks with perfect reconstruction using hybrid harmony-gravitational search algorithm," *Engineering Science and Technology, an International Journal*, vol. 18, no. 4, pp. 648–657, 2015.

[9] A. Shahein, Q. Zhang, N. Lotze, and Y. Manoli, "A novel hybrid monotonic local search algorithm for FIR filter coefficients optimization," *IEEE Transactions on Circuits and Systems I: Regular Papers*, vol. 59, no. 3, pp. 616–627, 2011. [Online]. Available: https://doi.org/10.1109/TCSI.2011.2165409

[10] Y. Cao, K. Wang, W. Pei, Y. Liu, and Y. Zhang, "Design of high-order extrapolated impulse response FIR filters with signed powers-of-two coefficients," *Circuits, Systems, and Signal Processing*, vol. 30, no. 5, pp. 963–985, 2011. [Online]. Available: https://doi.org/10.1007/s00034-010-9259-4

[11] V. Sakthivel, R. Chandru, and E. Elias, "Design of multiplier-less MDFT filter banks with perfect reconstruction using ABC algorithm," *International Journal of Computer Applications*, vol. 96, no. 1, 2014.

[Online]. Available: https://doi.org/10.1016/j.jestch.2015.03.012

[12] T. Bindiya, V. S. Kumar, and E. Elias, "Design of low power and low complexity multiplier-less reconfigurable non-uniform channel filter using genetic algorithm," *Glob. J. Res. Eng*, vol. 12, no. 6, pp. 7–19, 2012. [Online]. Available: https://doi.org/10.1145/3277453.3277470

[13] W. Xu, A. Li, R. Zhang, and B. Shi, "Efficient design of sparse multiplierless fir filters with low complexity," in *Proceedings of the 2018 International Conference on Electronics and Electrical Engineering Technology*, 2018, pp. 79–83. [Online]. Available: https://doi.org/10.1145/3277453.3277470

[14] A. Parvathi and V. Sakthivel, "Low complexity reconfigurable modified frm architecture with full spectral utilization for efficient channelizers," *Engineering Science and Technology, an International Journal*, 2021. [Online]. Available: https://doi.org/10.1016/j.jestch.2021.06.002

[15] R. Caetano, E. A. da Silva, and A. G. Ciancio, "Video coding using greedy decompositions on generalised bit-planes," *Electronics Letters*, vol. 38, no. 11, pp. 507–508, 2002. [Online]. Available: https://doi.org/10.1049/el:20020357

[16] K. K. Parhi, *VLSI digital signal processing systems: design and implementation*. John Wiley & Sons, 2007.

[17] F. Xu, C. H. Chang, and C. C. Jong, "Design of low-complexity FIR filters based on signed-powers-of-two coefficients with reusable common subexpressions," *IEEE Transactions on Computer-Aided Design of Integrated Circuits and Systems*, vol. 26, no. 10, pp. 1898–1907, 2007. [Online]. Available: https://doi.org/10.1109/TCAD.2007.895615

[18] Y. Neuvo, D. Cheng-Yu, and S. Mitra, "Interpolated finite impulse response filters," *IEEE Transactions on Acoustics, Speech, and Signal Processing*, vol. 32, no. 3, pp. 563–570, 1984. [Online]. Available: https://doi.org/10.1109/TASSP.1984.1164348

[19] I. Raghu and E. Elias, "Low complexity spectrum sensing technique for cognitive radio using farrow structure digital filters," *Engineering Science and Technology, an International Journal*, vol. 22, no. 1, pp. 131–142, 2019. [Online]. Available: https://doi.org/10.1016/j.jestch.2018.04.012

[20] E. A. da Silva, L. Lovisolo, A. J. Dutra, and P. S. Diniz, "FIR filter design based on successive approximation of vectors," *IEEE transactions on signal processing*, vol. 62, no. 15, pp. 3833–3848, 2014. [Online]. Available: https://doi.org/10.1109/TSP.2014.2324992

[21] K. Shaeen and E. Elias, "Prototype filter design approaches for near perfect reconstruction cosine modulated filter banks-a review," *Journal of Signal Processing Systems*, vol. 81, no. 2, pp. 183–195, 2015. [Online]. Available: https://doi.org/10.1007/s11265-014-0929-5

[22] V. Sakthivel and E. Elias, "Low complexity reconfigurable channelizers using non-uniform filter banks," *Computers & Electrical Engineering*, vol. 68, pp. 389–403, 2018. [Online]. Available: https://doi.org/10.1016/j.compeleceng.2018.04.015

[23] D. Li, Y. C. Lim, Y. Lian, and J. Song, "A polynomial-time algorithm for designing FIR filters with power-of-two coefficients," *IEEE Transactions on Signal Processing*, vol. 50, no. 8, pp. 1935–1941, 2002. [Online]. Available: https://doi.org/10.1109/TSP.2002.800385

[24] T. Bindiya and E. Elias, "Design of multiplier-less sharp transition width mdft filter banks using modified metaheuristic algorithms," *International Journal of Computer Applications*, vol. 88, no. 2, 2014. [Online]. Available: https://doi.org/10.5120/15321-3642